

Analytic model of elastic metamaterials with local resonances

Xiaoming Zhou and Gengkai Hu*

School of Aerospace Engineering, Beijing Institute of Technology, Beijing 100081, People's Republic of China

(Received 6 January 2009; revised manuscript received 6 April 2009; published 12 May 2009)

A unified analytic model for effective mass density, effective bulk modulus, and effective shear modulus is presented for elastic metamaterials composed of coated spheres embedded in a host matrix. The effective material properties are derived directly from the averages of local momentum, stress, and strain defined in a single doubly coated sphere. It is shown that the effective material parameters predicted by the proposed model are in excellent agreements with the coherent-potential approximation results at low filling fractions where the anisotropy of periodic structures can be neglected for elastic waves. The advantage of the proposed method is that it can reveal clearly the physical mechanism for negative effective material parameters induced by the resonant effect. It is found that negative effective mass density is induced by negative total momentum of the composite for a *positive momentum* excitation. Negative effective bulk modulus appears for composites with an increasing (decreasing) total volume under a compressive (tensile) stress. Negative effective shear modulus describes composites with axisymmetric deformation under an opposite axisymmetric loading. Numerical examples are also given to illustrate these mechanisms. These findings may be useful in design of elastic metamaterials.

DOI: [10.1103/PhysRevB.79.195109](https://doi.org/10.1103/PhysRevB.79.195109)

PACS number(s): 43.20.+g, 43.35.+d, 43.40.+s

I. INTRODUCTION

Recently, there has been a growing interest in analyzing the property of elastic metamaterials,^{1–8} which are the elastic wave counterparts of electromagnetic (EM) metamaterials.^{9–11} Generally speaking, metamaterials are composites whose building block can exhibit a resonance under wave excitation. When the building units are much smaller than the operating wavelength, the metamaterial can be homogenized as a material with negative effective material parameters, which are not readily realized in nature. For EM metamaterials, the physical mechanisms of achieving negative permittivity and negative permeability have been explained clearly by the fact that the building resonators will produce out-of-phase electric and magnetic polarizations.⁹ However the physical pictures on negative effective material parameters for elastic metamaterials are not very clearly demonstrated.

An isotropic elastic material is completely described through its mass density, bulk modulus, and shear modulus. In 2000, Liu *et al.*¹ fabricated a phononic crystal by putting the rubber-coated lead spheres in an epoxy matrix. Two phononic band gaps were observed in the long-wavelength regime and later found to be induced by negative effective mass density of the phononic crystal slab.¹² This phenomenon has been found in other elastic periodic mediums.^{13–15} The physical mechanism of negative effective mass density can be well understood with help of a simple mass-spring structure.^{16,17} The negative effective mass density arises from the negative total momentum of the unit cell with positive velocity fields due to local resonance, which has been confirmed by a recent experiment.¹⁸ Many works^{19–21} have been conducted to establish the equivalence between the actual composite and corresponding discrete mass-spring structure. The concept of negative-mass band gap has been utilized to control flexural vibrations of Timoshenko²² or Euler-Bernoulli²³ beams and near-total reflections of acoustic waves by a membrane-type composite.⁴

Negative effective modulus of elastic metamaterials is distinct from the negative static stiffness observed in the buckling state of compressed structures.²⁴ The former is induced by the local resonant effect, as demonstrated in a hollow waveguide attached by an array of subwavelength Helmholtz resonators.^{2,25} The effective compliance of Helmholtz resonators, the inverse of effective modulus, is found to have the Lorentz form, showing an interesting correlation with effective permeability of magnetic resonators.²⁶ This analogy enables one to understand the negative modulus from a simple inductor-capacitor circuit. By inducing the monopolar resonance of bubble-contained-water spheres in an epoxy host, Ding *et al.*³ also proposed a composite with a negative effective bulk modulus, which facilitates the fabrication of acoustic left-handed metamaterials.²⁷ Wu *et al.*²⁸ designed a fiber composite with a negative effective shear modulus by introducing the quadrupolar resonance.

The effective-medium theory based on the coherent-potential approximation (CPA) (Refs. 3 and 28–30) has usually been utilized to predict effective material parameters of specific periodic structures and can successfully predict the band structure of composite materials in a low filling fraction. However, the underlying physical mechanisms for negative-mass density, negative bulk modulus and negative shear modulus are not well demonstrated by this model. Taking a phononic crystal of rubber-coated lead spheres in an epoxy as a prototype, Liu *et al.*¹² made an important step in correlating the macroscopic averaging fields with the localized resonant mechanisms. In their model, the negative effective mass density is clearly shown to come from the out-of-phase effect between the momentum and velocity for the rubber-coated lead sphere cell. However their analytic method is not able to describe the physical mechanism of the second band gap induced by the out-of-phase movement of the rubber coating with respect to the epoxy host. Inspired by the analytic model proposed by Liu *et al.*,¹² we will further examine the physical mechanisms of the negative bulk and shear modulus for a composite consisting of coated spheres

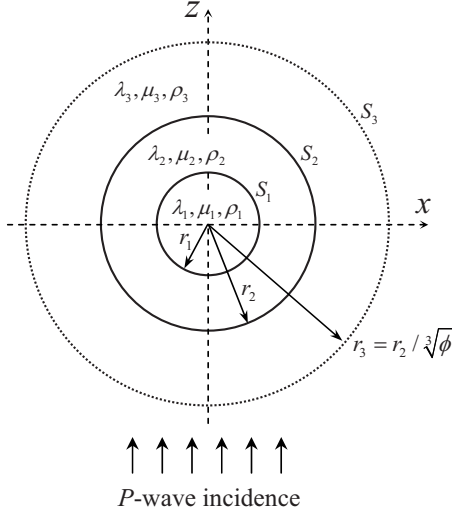


FIG. 1. A coated sphere radiated by a plane P wave. (The outer boundary of radius $r_3 = r_2 / \sqrt[3]{\phi}$ for the host material is defined according to the volume fraction ϕ occupied by the coated spheres in the composite)

embedded in a solid matrix. We present in Sec. II a unified analytic model for effective mass density, effective bulk modulus, and effective shear modulus of the composite. In Sec. III, comparisons will be provided between the proposed model and the CPA method for low filling fraction, where the anisotropy of periodic structures can be neglected. The physical mechanisms for the negative bulk and shear moduli of the composite will be demonstrated. Finally, the conclusion is given in Sec. IV.

II. ANALYTIC MODELS

The examined model consists of a three-phase composite with coated spheres embedded in a host material. The building unit is a doubly-coated sphere, as shown in Fig. 1, whose outer radius is defined by $r_3 = r_2 / \sqrt[3]{\phi}$, where ϕ is the filling fraction of the coated spheres. Each region of the doubly-coated sphere is assumed to be elastic material characterized by mass density ρ_i , Lamé coefficients λ_i and μ_i , and volume fractions ϕ_i with the subscript $i=1,2,3$ representing separately the sphere, the coating, and the host. Notice that $\phi = \phi_1 + \phi_2$. Let r_1 denote the radius of the uncoated sphere and r_2 the radius of the coated sphere. A plane harmonic compressional wave (P wave) propagates along the positive direction of the z axis, as shown in Fig. 1. The analytical solutions for the scattering displacement and stress fields of a coated sphere are given in the Appendix for later use.

A. Effective mass density

For a plane harmonic wave, the equation of motion for an elastic material is written as

$$\vec{\nabla} \cdot \vec{\sigma} = -i\omega \vec{p}. \quad (1)$$

Integrating Eq. (1) in a sphere with the volume V , the outer surface S , and the radius r , we can define the macroscopic equation of motion

$$\int_S d\vec{s} \cdot \vec{\sigma} = -i\omega V \langle \vec{p} \rangle, \quad (2)$$

where we have used the Green formula and the averaging momentum $\langle \vec{p} \rangle$ is defined as $\langle \vec{p} \rangle = \frac{1}{V} \int_V \vec{p} dv$. The integration in the left-hand side of Eq. (2) stands for the total force $\vec{F} = \int_S d\vec{s} \cdot \vec{\sigma}$ acting on the spherical surface S . Consider general expression (A7) of scattering stress fields of a spherical object, the total force is not zero only in the incident direction and given by

$$F_z = 4\pi \sum_n (\sigma'_{rr,n} l_n + \sigma'_{r\theta,n} m_n), \quad (3)$$

where

$$l_n = \int_{-1}^1 P_n(z) P_1(z) dz, \quad (4a)$$

$$m_n = \int_{-1}^1 P_n^1(z) P_1^1(z) dz, \quad (4b)$$

$$\sigma'_{rr,n} = \mu(E_n^{31} a_n + E_n^{32} b_n + E_n^{33} c_n + E_n^{34} d_n), \quad (5a)$$

$$\sigma'_{r\theta,n} = \mu(E_n^{41} a_n + E_n^{42} b_n + E_n^{43} c_n + E_n^{44} d_n). \quad (5b)$$

It is known that the Legendre polynomials $P_n^m(z)$ are orthogonal functions. Thus in Eq. (4) only l_1 and m_1 have nonvanishing values $l_1 = 2/3$ and $m_1 = 4/3$. It is noted that the total moment exerted by the surface stress is $\vec{M} = \int_S d\vec{s} \times \vec{\sigma}$. It is readily shown that $\vec{M} \equiv 0$, thus, the acoustic radiation will not rotate a sphere, i.e., the sphere has no angular momentum.

Based on Eq. (2), the macroscopic equations of motion for each region of a doubly coated sphere are written as

$$\int_{S_1} d\vec{s} \cdot \vec{\sigma} = -i\omega V_1 \langle \vec{p} \rangle_1, \quad (6a)$$

$$\int_{S_2} d\vec{s} \cdot \vec{\sigma} - \int_{S_1} d\vec{s} \cdot \vec{\sigma} = -i\omega V_2 \langle \vec{p} \rangle_2, \quad (6b)$$

$$\int_{S_3} d\vec{s} \cdot \vec{\sigma} - \int_{S_2} d\vec{s} \cdot \vec{\sigma} = -i\omega V_3 \langle \vec{p} \rangle_3, \quad (6c)$$

where S_1 , S_2 , and S_3 represent separately the sphere-coating interface $r=r_1$, the coating-matrix interface $r=r_2$, and the external surface $r=r_3$. V_i denotes the volume occupied by the i th region. With the total force F_z , we get the averaging momentum of each region as

$$\langle \vec{p} \rangle_1 = \frac{F_z(r_1)}{-i\omega V_1}, \quad (7a)$$

$$\langle \vec{p} \rangle_2 = \frac{F_z(r_2) - F_z(r_1)}{-i\omega V_2}, \quad (7b)$$

$$\langle \vec{p} \rangle_3 = \frac{F_z(r_3) - F_z(r_2)}{-i\omega V_3}. \quad (7c)$$

Since the velocity of the composite sphere that we observe is the velocity of the host material, we define the velocity of the composite as $\langle \vec{u} \rangle_{\text{total}} = \phi_3 \langle \vec{u} \rangle_3$. The total momentum of the composite is the sum of momentums of each region. Then according to the homogenization method, the dynamic effective mass density of the composite is defined as

$$\rho_{\text{eff}} = \frac{1}{4\pi r_3^3/3} \frac{\langle \vec{p} \rangle_{\text{total}}}{\langle \vec{u} \rangle_{\text{total}}} = \rho_3 \frac{\phi_1 \langle \vec{p} \rangle_1 + \phi_2 \langle \vec{p} \rangle_2 + \phi_3 \langle \vec{p} \rangle_3}{\langle \vec{p} \rangle_3}. \quad (8)$$

Substituting Eq. (7) into Eq. (8), we finally get

$$\begin{aligned} \rho_{\text{eff}} = & \phi_3 \rho_3 \{ [E_1^{31}(h, r_3) + 2E_1^{41}(h, r_3)] a_1^{(3)} + [E_1^{32}(h, r_3) \\ & + 2E_1^{42}(h, r_3)] b_1^{(3)} + 3i[E_1^{33}(h, r_3) \\ & + 2E_1^{43}(h, r_3)] \} / \{ [E_1^{31}(h, r_3) + 2E_1^{41}(h, r_3) - E_1^{31}(h, r_2) \\ & - 2E_1^{41}(h, r_2)] a_1^{(3)} + [E_1^{32}(h, r_3) + 2E_1^{42}(h, r_3) - E_1^{32}(h, r_2) \\ & - 2E_1^{42}(h, r_2)] b_1^{(3)} + 3i[E_1^{33}(h, r_3) + 2E_1^{43}(h, r_3) \\ & - E_1^{33}(h, r_2) - 2E_1^{43}(h, r_2)] \}, \quad (9) \end{aligned}$$

where E_1^{31} , E_1^{32} , E_1^{41} , and E_1^{42} are given by Eqs. (A10) and (A11) in the Appendix. $a_n^{(i)}$, $b_n^{(i)}$, $c_n^{(i)}$, and $d_n^{(i)}$ ($i=1, 2, 3$) are scattering coefficients in each region. The symbols “s,” “c,” and “h” represent the sphere, coating, and host, respectively, hereafter. In the long-wavelength limit, Eq. (9) reduces to the mixing law for solid materials

$$\rho_{\text{eff}}^s = \phi_1 \rho_1 + \phi_2 \rho_2 + \phi_3 \rho_3. \quad (10)$$

B. Effective bulk modulus

The constitutive relation for the i th region of the doubly-coated sphere is given by

$$\langle \vec{\sigma} \rangle_i = 3\lambda_i \langle \varepsilon_b \rangle_i \vec{I} + 2\mu_i \langle \vec{\varepsilon} \rangle_i, \quad (11)$$

where the averaging field $\langle \vec{\Gamma} \rangle_i$ is defined as $\langle \vec{\Gamma} \rangle_i = \frac{1}{V_i} \int_{V_i} \vec{\Gamma} dv$, $\varepsilon_b = \frac{1}{3} \text{tr} \vec{\varepsilon}$ is the bulk strain, and \vec{I} is the second-order unit

tensor. The strain tensor $\vec{\varepsilon}$ is related to the displacement field \vec{u} by

$$\varepsilon_b = \frac{1}{3} \vec{\nabla} \cdot \vec{u}, \quad (12)$$

$$\vec{\varepsilon} = \frac{1}{2} (\vec{\nabla} \vec{u} + \vec{u} \vec{\nabla}). \quad (13)$$

With help of the Green's formula and general expressions (A6) of the scattering displacement field, the averaging bulk strain $\langle \varepsilon_b \rangle_i$ is derived as

$$\langle \varepsilon_b \rangle_1 = \frac{2\pi}{3V_1} r_1^2 \sum_n u'_{r,n}(r_1) s_n, \quad (14a)$$

$$\langle \varepsilon_b \rangle_2 = \frac{2\pi}{3V_2} \sum_n [r_2^2 u'_{r,n}(r_2) - r_1^2 u'_{r,n}(r_1)] s_n, \quad (14b)$$

$$\langle \varepsilon_b \rangle_3 = \frac{2\pi}{3V_3} \sum_n [r_3^2 u'_{r,n}(r_3) - r_2^2 u'_{r,n}(r_2)] s_n, \quad (14c)$$

with

$$s_n = \int_{-1}^1 P_n(z) P_0(z) dz, \quad (15)$$

$$u'_{r,n}(r_i) = \frac{1}{r_i} (E_n^{11} a_n^{(i)} + E_n^{12} b_n^{(i)} + E_n^{13} c_n^{(i)} + E_n^{14} d_n^{(i)}). \quad (16)$$

In Eq. (15), only the nonzero value $s_0=2$ is obtained due to the orthogonal properties of Legendre polynomials $P_n(z)$. The averaging bulk strain $\langle \varepsilon_b \rangle_i$ describes the volume variations of the i th constituent. The volume will increase if $\langle \varepsilon_b \rangle_i > 0$ and decrease if $\langle \varepsilon_b \rangle_i < 0$.

The averaging bulk stress for the i th region $\langle \sigma_b \rangle_i = \frac{1}{3} \text{tr} \langle \vec{\sigma} \rangle_i$ can be calculated by

$$\langle \sigma_b \rangle_i = 3\kappa_i \langle \varepsilon_b \rangle_i, \quad (17)$$

where $\kappa_i = \lambda_i + \frac{2}{3} \mu_i$ is the bulk modulus. According to the homogenization method, the effective bulk modulus of the composite can be defined as

$$\kappa_{\text{eff}} = \frac{\langle \sigma_b \rangle_{\text{total}}}{3 \langle \varepsilon_b \rangle_{\text{total}}} = \frac{\kappa_1 \phi_1 \langle \varepsilon_b \rangle_1 + \kappa_2 \phi_2 \langle \varepsilon_b \rangle_2 + \kappa_3 \phi_3 \langle \varepsilon_b \rangle_3}{\phi_1 \langle \varepsilon_b \rangle_1 + \phi_2 \langle \varepsilon_b \rangle_2 + \phi_3 \langle \varepsilon_b \rangle_3}. \quad (18)$$

Substituting Eq. (14) into Eq. (18), we have

$$\kappa_{\text{eff}} = \kappa_3 + \frac{r_1(\kappa_1 - \kappa_2) E_0^{13}(s, r_1) c_0^{(1)} + r_2(\kappa_2 - \kappa_3) [E_0^{11}(h, r_2) a_0^{(3)} + E_0^{13}(h, r_2)]}{r_3 [E_0^{11}(h, r_3) a_0^{(3)} + E_0^{13}(h, r_3)]}, \quad (19)$$

where E_0^{11} and E_0^{13} are computed from Eq. (A8) in the Appendix. In the long-wavelength limit, Eq. (19) reduces to the static effective bulk modulus³¹ for a doubly-coated sphere assemblage

$$\kappa_{\text{eff}}^s = \kappa_3 + \frac{(\phi_1 + \phi_2)(\kappa'_{\text{eff}} - \kappa_3)}{1 + 3\phi_3(\kappa'_{\text{eff}} - \kappa_3)/(3\kappa_3 + 4\mu_3)}, \quad (20)$$

with

$$\kappa'_{\text{eff}} = \kappa_2 + \frac{\phi_1(\kappa_1 - \kappa_2)}{\phi_1 + \phi_2 + 3\phi_2(\kappa_1 - \kappa_2)/(3\kappa_2 + 4\mu_2)}. \quad (21)$$

C. Effective shear modulus

Now going back to Eq. (11) and considering the deviatoric part $\langle \tilde{\varepsilon}' \rangle_i$ of the averaging strain $\langle \tilde{\varepsilon} \rangle_i$, it can be expressed as

$$\langle \tilde{\varepsilon}' \rangle_i = \varepsilon''_i \begin{bmatrix} -1 & 0 & 0 \\ 0 & -1 & 0 \\ 0 & 0 & 2 \end{bmatrix}, \quad (22)$$

where

$$\varepsilon''_1 = \frac{\pi}{3V_1} r_1^2 \sum_n [2u'_{r,n}(r_1)p_n + u'_{\theta,n}(r_1)q_n], \quad (23a)$$

$$\varepsilon''_2 = \frac{\pi}{3V_2} \sum_n \{r_2^2[2u'_{r,n}(r_2)p_n + u'_{\theta,n}(r_2)q_n] - r_1^2[2u'_{r,n}(r_1)p_n + u'_{\theta,n}(r_1)q_n]\}, \quad (23b)$$

$$\varepsilon''_3 = \frac{\pi}{3V_3} \sum_n \{r_3^2[2u'_{r,n}(r_3)p_n + u'_{\theta,n}(r_3)q_n] - r_2^2[2u'_{r,n}(r_2)p_n + u'_{\theta,n}(r_2)q_n]\}, \quad (23c)$$

with

$$\mu_{\text{eff}} = \mu_3 + \frac{(\mu_1 - \mu_2)r_1^2[u'_{r,2}(r_1) + 3u'_{\theta,2}(r_1)] + (\mu_2 - \mu_3)r_2^2[u'_{r,2}(r_2) + 3u'_{\theta,2}(r_2)]}{r_3^2[u'_{r,2}(r_3) + 3u'_{\theta,2}(r_3)]}, \quad (30)$$

with

$$u'_{r,2}(r_1) = \frac{1}{r_1} [E_2^{13}(s, r_1)c_2^{(1)} + E_2^{14}(s, r_1)d_2^{(1)}], \quad (31a)$$

$$u'_{\theta,2}(r_1) = \frac{1}{r_1} [E_2^{23}(s, r_1)c_2^{(1)} + E_2^{24}(s, r_1)d_2^{(1)}], \quad (31b)$$

$$p_n = \int_{-1}^1 P_n(z)P_2(z)dz, \quad (24a)$$

$$q_n = \int_{-1}^1 P_n^1(z)P_2^1(z)dz. \quad (24b)$$

$$u'_{\theta,n}(r_i) = \frac{1}{r_i} (E_n^{21}a_n^{(i)} + E_n^{22}b_n^{(i)} + E_n^{23}c_n^{(i)} + E_n^{24}d_n^{(i)}). \quad (25)$$

Due to the orthogonal properties of Legendre polynomials $P_n^m(z)$, the nonvanishing values in Eq. (24) are $p_2=2/5$ and $q_2=12/5$, respectively. The angular distribution of forces acting on a sphere is determined by the second-order Legendre polynomials $P_2(\cos \theta)$. It is found from the total force that the sphere is under on average an axisymmetric loading, i.e., pulled in z direction and compressed equally in x - y plane, or vice versa. From the constitutive equation, the averaging deviatoric stress $\langle \tilde{\sigma}' \rangle$ is related to the deviatoric strain through the shear modulus of the i th region

$$\langle \tilde{\sigma}' \rangle_i = 2\mu_i \langle \tilde{\varepsilon}' \rangle_i, \quad (26)$$

or equivalently,

$$\langle \tau \rangle_i = 2\mu_i \langle e \rangle_i, \quad (27)$$

where the averaging shear strain $\langle e \rangle_i$ is defined as

$$\langle e \rangle_i = \frac{1}{2} [2\varepsilon''_i - (-\varepsilon''_i)] = \frac{3}{2} \varepsilon''_i, \quad (28)$$

and $\langle \tau \rangle_i$ is the corresponding averaging shear stress in the i th region.

According to the homogenization method, the effective shear modulus of the composite can be defined as

$$\mu_{\text{eff}} = \frac{\langle \tau \rangle_{\text{total}}}{2\langle e \rangle_{\text{total}}} = \frac{\mu_1\phi_1\langle e \rangle_1 + \mu_2\phi_2\langle e \rangle_2 + \mu_3\phi_3\langle e \rangle_3}{\phi_1\langle e \rangle_1 + \phi_2\langle e \rangle_2 + \phi_3\langle e \rangle_3}. \quad (29)$$

Substituting Eqs. (23) and (28) into Eq. (29), we obtain

$$u'_{r,2}(r_2) = \frac{1}{r_2} [E_2^{11}(h, r_2)a_2^{(3)} + E_2^{12}(h, r_2)b_2^{(3)} - 5E_2^{13}(h, r_2)], \quad (31c)$$

$$u'_{\theta,2}(r_2) = \frac{1}{r_2} [E_2^{21}(h, r_2)a_2^{(3)} + E_2^{22}(h, r_2)b_2^{(3)} - 5E_2^{23}(h, r_2)], \quad (31d)$$

$$u'_{r,2}(r_3) = \frac{1}{r_3} [E_2^{11}(h, r_3)a_2^{(3)} + E_2^{12}(h, r_3)b_2^{(3)} - 5E_2^{13}(h, r_3)], \quad (31e)$$

$$u'_{\theta,2}(r_3) = \frac{1}{r_3} [E_2^{21}(h, r_3)a_2^{(3)} + E_2^{22}(h, r_3)b_2^{(3)} - 5E_2^{23}(h, r_3)], \quad (31f)$$

where E_2^{ij} can be computed from Eqs. (A8) and (A9) in the Appendix. In the long-wavelength limit, Eq. (30) reduces to the static effective shear modulus³¹ of a doubly-coated sphere assemblage

$$\mu_{\text{eff}}^s = \mu_3 + \frac{5(\phi_1 + \phi_2)\mu_3(\mu'_{\text{eff}} - \mu_3)}{5\mu_3 + 6\phi_3(\mu'_{\text{eff}} - \mu_3)(\kappa_3 + 2\mu_3)/(3\kappa_3 + 4\mu_3)}, \quad (32)$$

with

$$\mu'_{\text{eff}} = \mu_2 + \frac{5\phi_1\mu_2(\mu_1 - \mu_2)}{5(\phi_1 + \phi_2)\mu_2 + 6\phi_2(\mu_1 - \mu_2)(\kappa_2 + 2\mu_2)/(3\kappa_2 + 4\mu_2)}. \quad (33)$$

So far, we have derived the effective mass density, bulk, and shear moduli of a composite with coated particles embedded in a host material. In the following, we will demonstrate by numerical examples the physical mechanisms for the negative effective material parameters induced by the local resonance.

III. NUMERICAL RESULTS AND DISCUSSIONS

It has long been pointed out³² that the propagation of elastic waves in a three-dimensional (3D) periodic structure is not isotropic. Thus effective methods should be carefully verified for specific periodicity of a 3D structure. However in the work given by Ni and Cheng,³³ it is found that the anisotropy factor can be very small for low filling fraction. Although the system that they examined is different from that in this work, we take the volume fraction of coated spheres as $\phi=5\%$ in all of the following examples and assume the anisotropy effect can be neglected. It is also important to note that we can further lower the filling fraction to make sure the assumption valid. The resonant effect that gives rise to negative effective material parameters still exists; however, the corresponding frequency band will become very narrow. But the conclusions, i.e., physical pictures of negative effective material parameters, made in this paper are not influenced. In the following, we will compare our results with the CPA methods, which can give a good prediction in the case of low filling fraction. According to the CPA method, the effective material parameters can be determined by imposing the total scatterings of a doubly-coated sphere embedded in the effective material to be vanishing. Let $a_n^{(3)}$ denote the external scattering coefficient of longitudinal waves for a coated sphere embedded in the matrix material. The CPA method leads to the following equations for computing the effective material parameters:

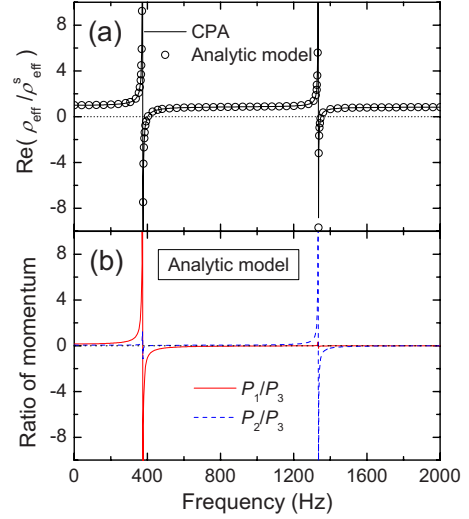


FIG. 2. (Color online) (a) The real parts of (a) effective mass density predicted by the CPA method and the analytic model and (b) the ratio of the averaging momentums P_1/P_3 and P_2/P_3 , where $P_i = \phi_i \langle p \rangle_i$.

$$\frac{\kappa_{\text{eff}} - \kappa_3}{3\kappa_{\text{eff}} + 4\mu_3} = \frac{a_0^{(3)}}{i(\alpha_3 r_3)^3}, \quad (34a)$$

$$\frac{\rho_{\text{eff}} - \rho_3}{\rho_3} = \frac{3a_1^{(3)}}{(\alpha_3 r_3)^3}, \quad (34b)$$

$$\frac{\mu_{\text{eff}} - \mu_3}{6\mu_{\text{eff}}(\kappa_3 + 2\mu_3) + \mu_3(9\kappa_3 + 8\mu_3)} = \frac{3ia_2^{(3)}}{20\mu_3(\alpha_3 r_3)^3}, \quad (34c)$$

where $\alpha_3 = \omega \sqrt{\rho_3 / (\lambda_3 + 2\mu_3)}$ is the longitudinal wave number in the host material.

We first examine a phononic crystal consisting of rubber-coated lead spheres embedded in an epoxy host.¹ The composite has been shown to exhibit a negative effective mass due to the dipolar resonance of the coated spheres. The material parameters used are $\rho_1 = 11.6 \times 10^3$ kg/m³, $\lambda_1 = 4.23 \times 10^{10}$ N/m², and $\mu_1 = 1.49 \times 10^{10}$ N/m² for lead, $\rho_2 = 1.3 \times 10^3$ kg/m³, $\lambda_2 = 6 \times 10^5$ N/m², and $\mu_2 = 4 \times 10^4$ N/m² for silicone rubber, and $\rho_3 = 1.18 \times 10^3$ kg/m³, $\lambda_3 = 4.43 \times 10^9$ N/m², and $\mu_3 = 1.59 \times 10^9$ N/m² for epoxy. The radius of the sphere is 5.0 mm, and the coating thickness is 2.5 mm. Figure 2(a) shows the real part of the effective mass density normalized to the static one $\rho_{\text{eff}}/\rho_{\text{eff}}^s$ predicted by the CPA method and presented model, respectively. Excellent agreement between two methods can be observed from the figure. The two negative-mass bands take place around the resonant frequencies 374 Hz and 1333 Hz. Since the averaging momentum $P_i = \phi_i \langle p \rangle_i$ can describe the macroscopic movement of each constituent, we plot the ratios P_1/P_3 and P_2/P_3 in Fig. 2(b) to examine the resonant mechanisms of the constituents. It is seen from Fig. 2(b) that the first and second negative-mass bands are induced, respectively, by the negative momentums of the lead sphere and rubber coating with respect to the epoxy host. Notice that the negative mo-

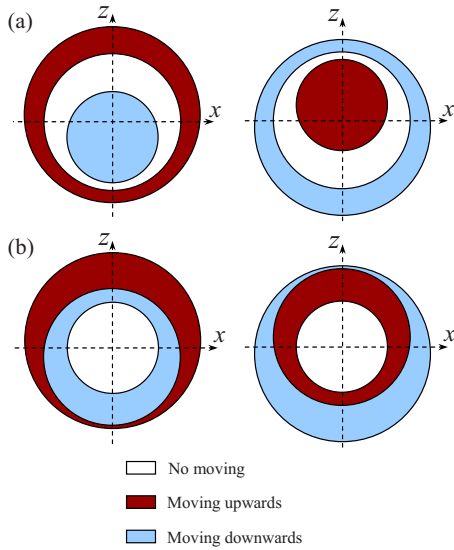


FIG. 3. (Color online) Schematic view of the displacement for a doubly-coated sphere at frequencies associated with (a) the first and (b) the second negative-mass bands.

mentum means the material will move in the opposite direction with the composite sphere. For better understanding, Figs. 3(a) and 3(b) show the schematic view for the movement of each region of a doubly-coated sphere at the frequencies associated with the first and second negative-mass bands, respectively. For simplicity, we further assume the rubber cover and lead sphere are at rest, respectively, in Figs. 3(a) and 3(b). Each constituent will oscillate along the incident direction since the total force is nonzero only in that direction. Figure 3(a) shows the out-of-phase movement of the inner sphere with respect to the composite sphere that is moving upwards or downwards. Due to the higher mass density and larger oscillation amplitude of the lead sphere than the epoxy matrix, the total momentum is opposite to the macroscopic velocity, then leading to the negative effective mass density. In Fig. 3(b), there is a similar phenomenon for the rubber coating moving in the opposite direction with respect to the composite sphere. Since its displacement amplitude is much larger than that of the composite sphere, the negative total momentum is again achieved, giving rise to the second negative-mass band. Based on the schematic plot shown in Fig. 3, equivalent mass-spring models can be easily constructed.^{17,18}

In the next example, we study the composite of bubble-contained-water spheres embedded in an epoxy matrix. The composite has been demonstrated to possess negative effective bulk modulus arising from the monopolar resonances of the inclusions.³ The material parameters are $\rho_1=1.23 \times 10^3 \text{ kg/m}^3$ and $\lambda_1=1.42 \times 10^5 \text{ N/m}^2$ for air and $\rho_2=1.0 \times 10^3 \text{ kg/m}^3$ and $\lambda_2=2.22 \times 10^9 \text{ N/m}^2$ for water. The radius of the sphere is 7.0 mm and the coating thickness is 73.0 mm. In Fig. 4(a), the real part of the effective bulk modulus calculated by the proposed model is shown in excellent agreements with the CPA results. Moreover, both methods predict a negative effective bulk modulus around the resonant frequency 1270 Hz. As we have indicated in Sec. II B, the averaging bulk strain is very important in describing a

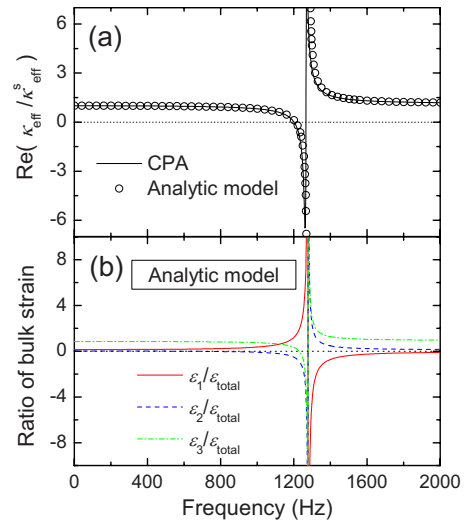


FIG. 4. (Color online) The real parts of (a) effective bulk modulus predicted by the CPA method and the analytic model and (b) the averaging bulk strains of each region versus the total bulk strain $\epsilon_1/\epsilon_{\text{total}}$, $\epsilon_2/\epsilon_{\text{total}}$, and $\epsilon_3/\epsilon_{\text{total}}$, where $\epsilon_i = \phi_i \langle \epsilon_b \rangle_i$ and $\epsilon_{\text{total}} = \sum_{i=1}^3 \phi_i \langle \epsilon_b \rangle_i$.

composite with unique effective bulk modulus. To explore the reason for the negative bulk modulus, the averaging bulk strains $\epsilon_i = \phi_i \langle \epsilon_b \rangle_i$ for the i th region normalized to the total bulk strain $\epsilon_{\text{total}} = \sum_{i=1}^3 \phi_i \langle \epsilon_b \rangle_i$ are presented in Fig. 4(b). If we examine the frequency at which $\epsilon_1/\epsilon_{\text{total}} > 0$, $\epsilon_2/\epsilon_{\text{total}} < 0$, and $\epsilon_3/\epsilon_{\text{total}} = 0$, the physical picture of negative effective bulk modulus can be well depicted in Fig. 5, which shows the schematic view of bulk deformations for the doubly-coated sphere in the expanding state [Fig. 5(b)] and the compressing state [Fig. 5(c)]. The doubly-coated sphere in the initial state without any deformation is shown in Fig. 5(a) for comparison. In the expanding state shown in Fig. 5(b), the inner core is greatly expanded due to the resonant effect so that the cover material is largely compressed and exhibiting a compressive stress. Since the bulk modulus of water is much larger than that of air, the loading state of the composite

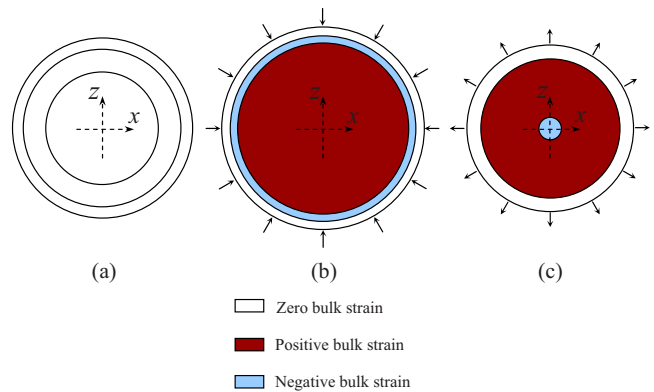


FIG. 5. (Color online) Schematic view of the deformation for a doubly-coated sphere when the composite sphere is (a) without deformation, (b) in the expanding state, and (c) in the compressing state. (The arrows indicate the directions of forces loading on the outermost surface of the composite sphere.)

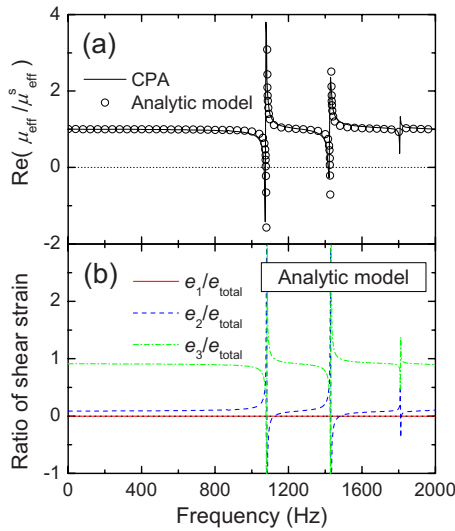


FIG. 6. (Color online) The real parts of (a) effective shear modulus predicted by the CPA method and the analytic model and (b) the averaging shear strains of each region versus the total shear strain e_1/e_{total} , e_2/e_{total} , and e_3/e_{total} , where $e_i = \phi_i \langle e \rangle_i$ and $e_{\text{total}} = \sum_{i=1}^3 \phi_i \langle e \rangle_i$.

sphere is completely governed by the water coating. Thus the composite sphere undergoes an expanding deformation under an external compressive stress. This effect needs to be described by a negative effective bulk modulus. In a similar sense, the composite sphere is under a tensile triaxial stress, but the total volume is decreasing, as shown in Fig. 5(c). So the negative effective bulk modulus arises from the out-of-phase volume deformation of local constituents compared to the external triaxial loading.

In the last example, we put rubber-coated epoxy spheres in the Polyethylene foam HD115. The material parameters of the Polyethylene foam are taken as $\rho_3 = 115 \text{ kg/m}^3$, $\lambda_3 = 6.0 \times 10^6 \text{ N/m}^2$, and $\mu_3 = 3.0 \times 10^6 \text{ N/m}^2$.³⁴ The radius of the epoxy sphere is 4.2 mm and the coating thickness is 5.4 mm. The real parts of effective shear modulus of the composite predicted by the CPA method and proposed model are shown in Fig. 6(a). It is seen that two methods predict negative effective shear modulus in two narrow frequency bands around 1082 Hz and 1428 Hz, respectively. In Sec. II C, we have indicated that the shear modulus results in an axisymmetric deformation for a doubly-coated sphere, which can be described by the averaging shear strain. To understand the mechanism of negative effective shear modulus, we plot in Fig. 6(b) the ratio of the averaging shear strains $e_i = \phi_i \langle e \rangle_i$ of the i th region to the total shear strain $e_{\text{total}} = \sum_{i=1}^3 \phi_i \langle e \rangle_i$ as a function of frequency. It is found from Fig. 6(b) that the averaging shear strain of the matrix can become negative, in correspondence with the negative effective shear modulus shown in Fig. 6(a). For further illustration, we assume a sphere will deform into a prolate or oblate spheroid of the constant volume under the axisymmetric loading. Figure 7 gives a schematic view for the deformation of a doubly-coated sphere when the negative effective shear modulus occurs. Figure 7(a) shows the doubly-coated sphere without any deformation for comparison. When the composite sphere (the outermost surface) deforms into a prolate shape, the

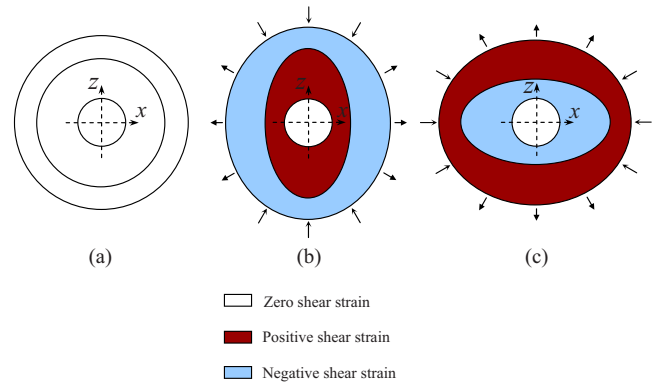


FIG. 7. (Color online) Schematic view of the deformation for a doubly-coated sphere when the composite sphere is (a) without deformation, (b) in the oblate-shape deformation, and (c) in the prolate-shape deformation. (The arrows indicate the directions of forces loading on the outermost surface of the composite sphere.)

cover material will also have a prolate shape but with a larger aspect ratio according to Fig. 6(b). The inner core has no shear deformation at any frequency. So the matrix cover is actually compressed in z direction and pulled in x - y plane, macroscopically behaving as the oblate-shape deformation. Since the Polyethylene foam is stiffer than the soft rubber, the composite sphere will be under the same loadings as the Polyethylene foam, as shown by the arrows in Fig. 7(b). The out-of-phase phenomenon between the deformation and the applied stress is the origin of negative effective shear modulus. A similar understanding can be given to the case in Fig. 7(c), where the composite sphere is compressed in z direction under a tensile stress and pulled out in x - y plane under a compressive stress.

Above numerical examples clearly demonstrate that the out-of-phase phenomenon induced by resonance is the origin of negative effective material parameters. The presented analytic model can give a unified explanation for this unusual phenomenon with help of the averaging physical fields. In addition, previous findings^{35,36} have revealed that the mass density, bulk modulus, and shear modulus dominate, respectively, the first three scattering channels in the long-wavelength limit. Here it is further found that the first three scattering channels correspond, respectively, to the rigid-body movement ($n=1$), the volume deformation ($n=0$), and the axisymmetric deformation of the constant volume ($n=2$). In this sense, the presented analytic method provides a useful tool in designing the microstructural resonance to get the unique macroscopic response. Additionally, the analytic model is likely to stimulate interesting applications of elastic metamaterials in the fields of ultrasonic subwavelength imaging,³⁷ elastic cloaking,^{36,38–40} and transformation acoustics.⁴¹

IV. CONCLUSIONS

Based on the Mie scattering solution, we present a unified analytic model to predict the dynamic effective material parameters for composites with coated particles by averaging physical fields from local constituents. For the low filling

fraction that the anisotropy of periodic structures can be neglected, the numerical results reveal that effective material parameters predicted by the proposed model agree well with those by the CPA method, even around the resonant frequencies at which effective material parameters may become negative. In addition, the analytic model can provide clear physical pictures for negative effective material parameters. Negative effective mass density arises from negative total momentums exhibited by the composite with positive velocity fields. Negative effective bulk modulus describes the composite with an increasing (decreasing) volume under a compressive (tensile) triaxial stress. Negative effective shear modulus describes the composite with axisymmetric deformation of the constant volume under the opposite axisymmetric loading. These findings may be helpful in designing elastic metamaterials and new band-gap phononic crystals.

ACKNOWLEDGMENTS

The authors thank Xiaoning Liu for helpful discussions. This work is supported by the National Natural Science Foundation of China (Grants No. 90605001, No. 10702006, and No. 10832002), the National Basic Research Program of China (Grant No. 2006CB601204), and Beijing Municipal Commission of Education Project (Grant No. 20080739027).

APPENDIX: SCATTERING SOLUTIONS OF AN ELASTIC COATED SPHERE

When a plane longitudinal wave is incident on a coated sphere along the positive z direction, as shown in Fig. 1, the potentials of longitudinal and shear waves in the l th region can be defined as⁴²

$$\Phi^{(l)} = \sum_{n=0}^{\infty} [c_n^{(l)} j_n(\alpha_l r) - a_n^{(l)} h_n(\alpha_l r)] P_n(\cos \theta), \quad (\text{A1a})$$

$$\Psi^{(l)} = \sum_{n=0}^{\infty} [d_n^{(l)} j_n(\beta_l r) - b_n^{(l)} h_n(\beta_l r)] P_n(\cos \theta), \quad (\text{A1b})$$

where $\alpha_l = \omega \sqrt{\rho_l / (\lambda_l + 2\mu_l)}$ and $\beta_l = \omega \sqrt{\rho_l / \mu_l}$, $j_n(x)$ is the spherical Bessel function of the first kind, $h_n(x)$ is the spherical Hankel function of first kind, and $P_n(x)$ is the Legendre polynomial.

The displacement vector can be expressed in terms of two potentials Φ and Ψ as

$$\vec{u} = \vec{\nabla} \Phi + \vec{\nabla} \times \left(\vec{e}_\varphi \frac{\partial \Psi}{\partial \theta} \right), \quad (\text{A2})$$

which gives

$$u_r = \frac{\partial \Phi}{\partial r} - r \beta^2 \Psi - 2 \frac{\partial \Psi}{\partial r} - r \frac{\partial^2 \Psi}{\partial r^2}, \quad (\text{A3a})$$

$$u_\theta = \frac{\partial}{\partial \theta} \left[\frac{1}{r} \Phi - \frac{1}{r} \Psi - \frac{\partial \Psi}{\partial r} \right], \quad (\text{A3b})$$

$$u_\phi = 0. \quad (\text{A3c})$$

The stress components are related to the displacements as

$$\vec{\sigma} = \lambda (\vec{\nabla} \cdot \vec{u}) \vec{I} + \mu (\vec{\nabla} \vec{u} + \vec{u} \vec{\nabla}). \quad (\text{A4})$$

From Eq. (A4), we have

$$\sigma_{rr} = -\lambda \alpha^2 \Phi + 2\mu \left[\frac{\partial^2 \Phi}{\partial r^2} - \beta^2 \Psi - r \beta^2 \frac{\partial \Psi}{\partial r} - 3 \frac{\partial^2 \Psi}{\partial r^2} - r \frac{\partial^3 \Psi}{\partial r^3} \right], \quad (\text{A5a})$$

$$\sigma_{r\theta} = 2\mu \frac{\partial}{\partial \theta} \left[-\frac{1}{r^2} \Phi + \frac{1}{r} \frac{\partial \Phi}{\partial r} + \frac{1}{r^2} \left(1 - \frac{\beta^2 r^2}{2} \right) \Psi - \frac{1}{r} \frac{\partial \Psi}{\partial r} - \frac{\partial^2 \Psi}{\partial r^2} \right], \quad (\text{A5b})$$

$$\sigma_{r\phi} = 0. \quad (\text{A5c})$$

By the substitution of Eq. (A1) into Eqs. (A3) and (A5), the stress and displacement fields in each region are

$$u_r^l = \frac{1}{r} \sum_n [E_n^{11} a_n^{(l)} + E_n^{12} b_n^{(l)} + E_n^{13} c_n^{(l)} + E_n^{14} d_n^{(l)}] P_n(\cos \theta), \quad (\text{A6a})$$

$$u_\theta^l = \frac{1}{r} \sum_n [E_n^{21} a_n^{(l)} + E_n^{22} b_n^{(l)} + E_n^{23} c_n^{(l)} + E_n^{24} d_n^{(l)}] \frac{dP_n(\cos \theta)}{d\theta}, \quad (\text{A6b})$$

$$\sigma_{rr}^l = \frac{2\mu_l}{r^2} \sum_n [E_n^{31} a_n^{(l)} + E_n^{32} b_n^{(l)} + E_n^{33} c_n^{(l)} + E_n^{34} d_n^{(l)}] P_n(\cos \theta), \quad (\text{A7a})$$

$$\sigma_{r\theta}^l = \frac{2\mu_l}{r^2} \sum_n [E_n^{41} a_n^{(l)} + E_n^{42} b_n^{(l)} + E_n^{43} c_n^{(l)} + E_n^{44} d_n^{(l)}] \frac{dP_n(\cos \theta)}{d\theta}, \quad (\text{A7b})$$

where $c_n^{(3)} = (2n+1)i^n$, $a_n^{(1)} = b_n^{(1)} = d_n^{(3)} = 0$, and

$$E_n^{11} = -nh_n(\alpha r) + \alpha r h_{n+1}(\alpha r), \quad (\text{A8a})$$

$$E_n^{12} = n(n+1)h_n(\beta r), \quad (\text{A8b})$$

$$E_n^{13} = nj_n(\alpha r) - \alpha r j_{n+1}(\alpha r), \quad (\text{A8c})$$

$$E_n^{14} = -n(n+1)j_n(\beta r), \quad (\text{A8d})$$

$$E_n^{21} = -h_n(\alpha r), \quad (\text{A9a})$$

$$E_n^{22} = (n+1)h_n(\beta r) - \beta r h_{n+1}(\beta r), \quad (\text{A9b})$$

$$E_n^{23} = j_n(\alpha r), \quad (\text{A9c})$$

$$E_n^{24} = -(n+1)j_n(\beta r) + \beta r j_{n+1}(\beta r). \quad (\text{A9d})$$

$$E_n^{31} = -(n^2 - n - \beta^2 r^2/2)h_n(\alpha r) - 2\alpha r h_{n+1}(\alpha r), \quad (\text{A10a})$$

$$E_n^{32} = n(n+1)[(n-1)h_n(\beta r) - \beta r h_{n+1}(\beta r)], \quad (\text{A10b})$$

$$E_n^{33} = (n^2 - n - \beta^2 r^2/2)j_n(\alpha r) + 2\alpha r j_{n+1}(\alpha r), \quad (\text{A10c})$$

$$E_n^{34} = -n(n+1)[(n-1)j_n(\beta r) - \beta r j_{n+1}(\beta r)], \quad (\text{A10d})$$

$$E_n^{41} = -(n-1)h_n(\alpha r) + \alpha r h_{n+1}(\alpha r), \quad (\text{A11a})$$

$$E_n^{42} = (n^2 - 1 - \beta^2 r^2/2)h_n(\beta r) + \beta r h_{n+1}(\beta r), \quad (\text{A11b})$$

$$E_n^{43} = (n-1)j_n(\alpha r) - \alpha r j_{n+1}(\alpha r), \quad (\text{A11c})$$

$$E_n^{44} = -(n^2 - 1 - \beta^2 r^2/2)j_n(\beta r) - \beta r j_{n+1}(\beta r). \quad (\text{A11d})$$

At the sphere-coating interface $r=r_1$ and the external surface $r=r_2$, the normal and tangential components of the displacements and stresses should be continuous. Eight equations can be constructed to solve uniquely all unknown scattering coefficients.

*Author to whom correspondence should be addressed; hugeng@bit.edu.cn

¹Z. Y. Liu, X. Zhang, Y. Mao, Y. Y. Zhu, C. T. Chan, and P. Sheng, *Science* **289**, 1734 (2000).

²N. Fang, D. Xi, J. Xu, M. Ambati, W. Srituravanich, C. Sun, and X. Zhang, *Nature Mater.* **5**, 452 (2006).

³Y. Q. Ding, Z. Y. Liu, C. Y. Qiu, and J. Shi, *Phys. Rev. Lett.* **99**, 093904 (2007).

⁴Z. Yang, J. Mei, M. Yang, N. H. Chan, and P. Sheng, *Phys. Rev. Lett.* **101**, 204301 (2008).

⁵S. Guenneau, A. Movchan, G. Pétursson, and S. A. Ramakrishna, *New J. Phys.* **9**, 399 (2007).

⁶D. Torrent and S. José, *New J. Phys.* **9**, 323 (2007).

⁷D. Torrent and S. José, *New J. Phys.* **10**, 023004 (2008).

⁸X. Hu, K. M. Ho, C. T. Chan, and Z. Jian, *Phys. Rev. B* **77**, 172301 (2008).

⁹D. R. Smith, J. B. Pendry, and M. C. K. Wiltshire, *Science* **305**, 788 (2004).

¹⁰J. B. Pendry, *Contemp. Phys.* **45**, 191 (2004).

¹¹S. A. Ramakrishna, *Rep. Prog. Phys.* **68**, 449 (2005).

¹²Z. Liu, C. T. Chan, and P. Sheng, *Phys. Rev. B* **71**, 014103 (2005).

¹³Z. Liu, C. T. Chan, and P. Sheng, *Phys. Rev. B* **65**, 165116 (2002).

¹⁴G. Wang, X. Wen, J. Wen, L. Shao, and Y. Liu, *Phys. Rev. Lett.* **93**, 154302 (2004).

¹⁵H. Larabi, Y. Pennec, B. Djafari-Rouhani, and J. O. Vasseur, *Phys. Rev. E* **75**, 066601 (2007).

¹⁶A. B. Movchan and S. Guenneau, *Phys. Rev. B* **70**, 125116 (2004).

¹⁷G. W. Milton and J. R. Willis, *Proc. R. Soc. London, Ser. A* **463**, 855 (2007).

¹⁸S. S. Yao, X. M. Zhou, and G. K. Hu, *New J. Phys.* **10**, 043020 (2008).

¹⁹C. Goffaux, J. Sanchez-Dehesa, A. Levy Yeyati, Ph. Lambin, A. Khelif, J. O. Vasseur, and B. Djafari-Rouhani, *Phys. Rev. Lett.* **88**, 225502 (2002); C. Goffaux and J. Sánchez-Dehesa, *Phys. Rev. B* **67**, 144301 (2003).

²⁰M. Hirsekorn, *Appl. Phys. Lett.* **84**, 3364 (2004).

²¹M. Hirsekorn, P. P. Delsanto, A. C. Leung, and P. Matic, *J. Appl. Phys.* **99**, 124912 (2006).

²²D. L. Yu, Y. Z. Liu, G. Wang, H. G. Zhao, and J. Qiu, *J. Appl. Phys.* **100**, 124901 (2006).

²³D. L. Yu, Y. Z. Liu, H. G. Zhao, G. Wang, and J. Qiu, *Phys. Rev. B* **73**, 064301 (2006).

²⁴R. S. Lakes, T. Lee, A. Bersie, and Y. C. Wang, *Nature (London)* **410**, 565 (2001).

²⁵Z. G. Wang, S. H. Lee, C. K. Kim, C. M. Park, K. Nahm, and S. A. Nikitov, *J. Appl. Phys.* **103**, 064907 (2008).

²⁶J. B. Pendry, A. J. Holden, D. J. Robbins, and W. J. Stewart, *IEEE Trans. Microwave Theory Tech.* **47**, 2075 (1999).

²⁷J. Li and C. T. Chan, *Phys. Rev. E* **70**, 055602 (2004).

²⁸Y. Wu, L. Yun, and Z. Q. Zhang, *Phys. Rev. B* **76**, 205313 (2007).

²⁹P. Sheng, *Introduction to Wave Scattering, Localization, and Mesoscopic Phenomena* (Academic, San Diego, 1995).

³⁰A. Modinos, V. Yannopoulos, and N. Stefanou, *Phys. Rev. B* **61**, 8099 (2000).

³¹G. W. Milton, *The Theory of Composites* (Cambridge University Press, Cambridge, England, 2002).

³²L. D. Landau and E. M. Lifshitz, *Theory of Elasticity*, 3rd ed. (Butterworth-Heinemann, Oxford, 1986).

³³Q. Ni and J. C. Cheng, *J. Appl. Phys.* **101**, 073515 (2007).

³⁴C. E. S. Selector 4.0 (<http://www.grantadesign.com/products/ces/>).

³⁵J. Mei, Z. Y. Liu, W. J. Wen, and P. Sheng, *Phys. Rev. Lett.* **96**, 024301 (2006).

³⁶X. M. Zhou, G. K. Hu, and T. J. Lu, *Phys. Rev. B* **77**, 024101 (2008).

³⁷M. Ambati, N. Fang, C. Sun, and X. Zhang, *Phys. Rev. B* **75**, 195447 (2007).

³⁸G. W. Milton, M. Briane, and J. R. Willis, *N. J. Phys.* **8**, 248 (2006).

³⁹M. Brun, S. Guenneau, and A. B. Movchan, *Appl. Phys. Lett.* **94**, 061903 (2009).

⁴⁰M. Farhat, S. Guenneau, S. Enoch, and A. B. Movchan, *Phys. Rev. B* **79**, 033102 (2009).

⁴¹H. Chen and C. T. Chan, *Appl. Phys. Lett.* **91**, 183518 (2007).

⁴²Y. H. Pao and C. C. Mow, *Diffraction of Elastic Waves and Dynamic Stress Concentrations* (Crane and Russak, New York, 1973).